Interaction of Zn(II)·Bleomycin with d(CGCTAGCG)$_2$. A Binding Model Based on NMR Experiments and Restrained Molecular Dynamics Calculations

Richard A. Manderville,† Jeffrey F. Ellena,† and Sidney M. Hecht*,‡

Contribution from the Departments of Chemistry and Biology, University of Virginia, Charlottesville, Virginia 22901

Received March 15, 1995[⊗]

Abstract: The antitumor antibiotic bleomycin (BLM) binds to and degrades the self-complementary octanucleotide d(CGCTAGCG)$_2$ in a sequence-selective fashion. To model the binding interaction, 1:1 complexes of Zn(II)·BLM A_2 and Zn(II)·BLM A_5 with the DNA oligonucleotide have been examined using two-dimensional NMR experiments and restrained molecular dynamics calculations. Intercalation is indicated by the broadening and upfield shifting of the BLM aromatic bithiazole protons and DNA base-paired imino protons. However, the data do not support a classical mode of intercalation, as the sequential intrastrand NOE connectivities of d(CGCTAGCG)$_2$ are not disrupted upon Zn·BLM binding. The orientation of the drug molecule in the helix is based on the finding of eight intermolecular BLM−DNA NOEs in the Zn·BLM A_5−d(CGCTAGCG)$_2$ complex. The bithiazole B-ring proton (Bit 5) and spermidine H3 (Sp 3) atoms are positioned within 5 Å of adenosine$_5$ H2 in the minor groove, while the bithiazole A-ring proton (Bit 5′) shows major groove contacts to protons of cytidine$_3$ and thymidine$_4$. Protons of the β-hydroxyhistidine and methyl valerate residues show minor groove contacts (H4′ and H5′,5″) to cytidine$_7$. Using the NMR-derived NOE distance and dihedral bond angle restraints to guide the molecular dynamics calculations, a binding model for the interaction of Zn·BLM with the octanucleotide was derived. To satisfy the major and minor groove BLM-DNA NOE contacts, this model positions the bithiazole ring system in a "*cis*" orientation (H atoms on same side) with the H atoms directed into the helix. Such an orientation favors partial stacking interactions between the DNA bases and the bithiazole rings and permits interaction of the cationic spermidine tail and metal binding domain with the minor groove of the helix. The upfield shifts observed for the bithiazole aromatic protons are in agreement with the effects predicted for protons oriented as in the model. The BLM molecule adopts a folded conformation that favors H bond formation between the exocyclic NH_2 group of guanosine$_6$ and the hydroxyl group of the methyl valerate residue. This binding mode involves DNA unwinding, which widens the minor groove, as well as a bend in the helix that is induced at the bithiazole binding site. The DNA unwinding angle of 13° calculated for this model is in good agreement with the experimentally determined value of 12°. The validity of this DNA binding model and possible implications for sequence-selective cleavage by BLM are discussed. Also discussed is the effect of DNA sequence on the nature of BLM−DNA interaction.

The bleomycins (BLMs) are a family of glycopeptide-derived antitumor antibiotics originally isolated from a fermentation broth of *Streptomyces verticillus*.[1] A mixture of BLMs is employed clinically for the treatment of squamous cell carcinomas, testicular tumors, and malignant lymphomas.[2] Their therapeutic effects are believed to derive from their ability to effect the degradation of DNA,[3] and possibly RNA,[4] in the presence of O_2 and a redox-active metal ion such as Fe[5] or Cu.[6] The structure of bleomycin (Figure 1) is commonly divided into functional domains. The N-terminus, or metal binding domain, is responsible for metal binding, oxygen binding and activation as well as DNA binding.[7] The disaccharide moiety also participates in metal ion binding[8] and may additionally be involved in cell surface recognition.[4d] The C-terminus, comprised of the bithiazole (Bit) and cationic substituent (sulfonium (Sul) in BLM A_2, spermidine (Sp) in BLM A_5, Figure 1) participates in DNA binding.[9]

Sequence-selective DNA damage by bleomycin involves drug

† Department of Chemistry.

‡ Departments of Chemistry and Biology.

⊗ Abstract published in *Advance ACS Abstracts*, July 1, 1995.

(1) Umezawa, H.; Suhara, Y.; Takita, T.; Maeda, K. *J. Antibiot.* **1966**, *19A*, 210.

(2) *Bleomycin Chemotherapy*; Sikic, B. I.; Rozencweig, M.; Carter, S. K., Eds.; Academic Press: Orlando, FL, 1985.

(3) (a) D'Andrea, A. D.; Haseltine, W. A. *Proc. Natl. Acad. Sci. U.S.A.* **1978**, *75*, 3608. (b) Takeshita, M.; Grollman, A. P.; Ohtsubo, E.; Ohtsubo, H. *Proc. Natl. Acad. Sci. U.S.A.* **1978**, *75*, 5983. (c) Mirabelli, C. K.; Huang, C.-H.; Crooke, S. T. *Biochemistry* **1983**, *22*, 300.

(4) (a) Carter, B. J.; de Vroom, E.; Long, E. C.; van der Marel, G. A.; van Boom, J. H.; Hecht, S. M. *Proc. Natl. Acad. Sci. U.S.A.* **1990**, *87*, 9373. (b) Holmes, C. E.; Carter, B. J.; Hecht, S. M. *Biochemistry* **1993**, *32*, 4293. (c) Morgan, M. A.; Hecht, S. M. *Biochemistry* **1994**, *33*, 10286. (d) Hecht, S. M. *Bioconjugate Chem.* **1994**, *5*, 513.

(5) (a) Ishida, R.; Takahashi, T. *Biochem. Biophys. Res. Commun.* **1975**, *66*, 1432. (b) Sausville, E. A.; Peisach, J.; Horwitz, S. B. *Biochemistry* **1978**, *17*, 2740. (c) Sausville, E. A.; Stein, R. W.; Peisach, J.; Horwitz, S. B. *Biochemistry* **1978**, *17*, 2746.

(6) (a) Ehrenfeld, G. M.; Rodriguez, L. O; Hecht, S. M.; Chang, C.; Basus, V. J.; Oppenheimer, N. J. *Biochemistry* **1985**, *24*, 81. (b) Ehrenfeld, G. M.; Shipley, J. B.; Heimbrook, D. C.; Sugiyama, H.; Long, E. C.; van Boom, J. H., van der Marel, G. A.; Oppenheimer, N. J.; Hecht, S. M. *Biochemistry* **1987**, *26*, 931.

(7) (a) Carter, B. J.; Murty, V. S.; Reddy, K. S.; Wang, S.-N.; Hecht, S. M. *J. Biol. Chem.* **1990**, *265*, 4193. (b) Guajardo, R. J.; Hudson, S. E.; Brown, S. J.; Mascharak, P. K. *J. Am. Chem. Soc.* **1993**, *115*, 7971.

(8) (a) Oppenheimer, N. J.; Rodriguez, L. O.; Hecht, S. M. *Proc. Natl. Acad. Sci. U.S.A.* **1979**, *76*, 5616. (b) Akkerman, M. A. J.; Neijman, E. W. J. F.; Wijmenga, S. S.; Hilbers, C. W.; Bermel, W. *J. Am. Chem. Soc.* **1990**, *112*, 7462.

(9) (a) Hecht, S. M. *Acc. Chem. Res.* **1986**, *19*, 383. (b) Stubbe, J.; Kozarich, J. W. *Chem. Rev.* **1987**, *87*, 1107. (c) Natrajan, A.; Hecht, S. M. In *Molecular Aspects of Anticancer Drug-DNA Interactions*; Neidle, S.; Waring, M., Eds.; MacMillan: London, 1994; pp 197−242. (d) Kane, S. A.; Hecht, S. M. *Prog. Nucleic Acid Res. Mol. Biol.* **1994**, *49*, 313. (e) Hecht, S. M. In *Cancer Chemotherapeutic Agents*; Foye, W. O., Ed.; American Chemical Society: Washington, 1995; pp 369−388.

0002-7863/95/1517-7891$09.00/0

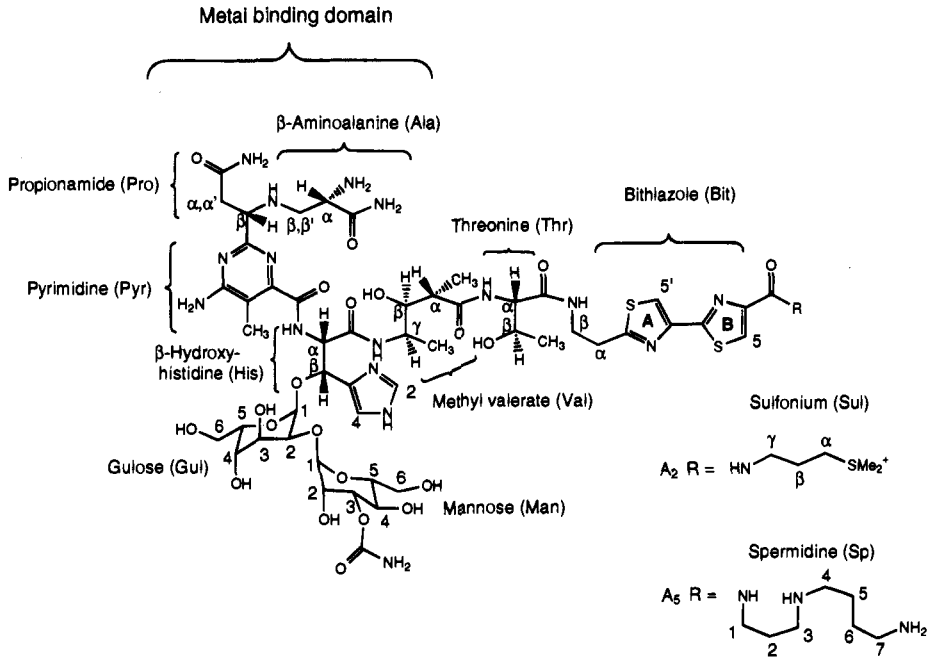

Figure 1. Structures of bleomycin A_2 and A_5 and designations for individual structural elements.

binding to DNA.[9] Bleomycin binds to double-stranded DNA with an apparent equilibrium constant of ca. 10^5 M^{-1};[10] the binding site size corresponds to 3−4 base pairs. Once bound, the drug is able to produce lesions in DNA that typically involve oxidative destruction of the pyrimidine nucleotides in 5′-GC-3′ and 5′-GT-3′ sequences.[9] Although the molecular basis for this specificity remains unresolved, it appears that the structural elements that determine sequence selectivity reside in the metal binding domain;[7,11] this domain must be positioned in the minor groove of the DNA substrate, since BLM-mediated DNA degradation is initiated by C4′ H atom abstraction from the sugar moieties.[12]

During the course of our studies of bleomycin-mediated DNA degradation, we have been particularly interested in the interaction of BLM with the self-complementary octanucleotide 5′-d(CGCTAGCG)-3′.[4d,9,13] Although this substrate is cleaved by Fe•BLM both at cytidine$_3$ and cytidine$_7$, modification at the latter site is strongly preferred.[13] The more facile abstraction of C4′ H from cytidine$_7$ is suggestive of a preferred binding orientation for BLM. To gain insight into this orientation, two-dimensional NMR techniques in conjunction with molecular dynamics calculations have been used to study the interaction of Zn(II)•bleomycin with the octanucleotide. This system constitutes a reasonable model for DNA binding by activated metallobleomycins.

Our initial study of the binding of Zn(II)•BLM A_5 to d(CGCTAGCG)$_2$ afforded NMR data that seemed to support both intercalation and minor groove binding by Zn(II)•BLM A_5.[14] Molecular dynamics calculations on the BLM structure with the octanucleotide approximated by a B-form conformation, i.e., in the absence of molecular dynamics calculations on the octamer, suggested a minor groove binding model with Zn(II)•BLM present in a folded conformation. Although the model represented a low energy structure consistent with the known chemistry of BLM[9] and the equilibrium binding data,[10] the source of the ring-current induced upfield shifts of the bithiazole aromatic resonances upon DNA binding was not readily apparent from this model.[14] Thus, it is evident that the interaction of the bithiazole moiety of BLM with DNA cannot be fully explained by a minor groove orientation where the bithiazole ring N atoms are hydrogen bonded to the guanosine NH_2 in the minor groove.

Presently, we report our more recent efforts to define the interaction of Zn•BLM with the octanucleotide d(CGCTAGCG)$_2$. Additional insight has been obtained by examining the complex of the octamer with Zn(II)•BLM A_2 (Figure 1, R = Sul). Further, by performing restrained molecular dynamics calculations on the entire Zn(II)•BLM A_5−d(CGCTAGCG)$_2$ complex as well as on the free octanucleotide we have been able to develop a model for Zn(II)•BLM binding to d(CGCTAGCG)$_2$ that is fully consistent with the NMR data obtained as well as all published biochemical data.

The final structures indicate that the Zn(II)•BLM is oriented primarily in the minor groove of the helix, with one ring of the bithiazole stacked between adjacent base pairs to varying extents in the set of structures on which our model is based. The stacking interaction results in a bend (kink) in the DNA structure.[15] All structures generated favor upfield shifting of the bithiazole aromatic protons since the bithiazole ring system is in a "*cis*" orientation (Figure 2) with the H atoms directed into the helix. The folded conformation of the drug permits the formation of a hydrogen bond between the exocyclic NH_2 group of guanosine$_6$ and the hydroxyl group of the methyl valerate (Val) residue. Comparison of the free versus bound

(10) (a) Chien, M.; Grollman, A. P.; Horwitz, S. B. *Biochemistry* **1977**, *16*, 3641. (b) Kasai, H.; Naganawa, H.; Takita, T.; Umezawa, H. *J. Antibiot.* **1978**, *31*, 1316. (c) Huang, C.-H.; Galvan, L.; Crooke, S. T. *Biochemistry* **1980**, *19*, 1761. (d) Povirk, L. F.; Hogan, M.; Dattagupta, N.; Buechner, M. *Biochemistry* **1981**, *20*, 665. (e) Roy, S. N.; Orr, G. A.; Brewer, C. F.; Horwitz, S. B. *Cancer Res.* **1981**, *41*, 4471. (f) Dabrowiak, J. C. *Adv. Inorg. Biochem.* **1982**, *4*, 70, and references therein. (g) Boger, D. L.; Colletti, S. L; Honda, T.; Menezes, R. F. *J. Am. Chem. Soc.* **1994**, *116*, 5607.

(11) (a) Sugiyama, H.; Kilkuskie, R. E.; Chang, L.-H.; Ma, L.-T.; Hecht, S. M.; van der Marel, G. A.; van Boom, J. H. *J. Am. Chem. Soc.* **1986**, *108*, 3852. (b) Kane, S. A.; Natrajan, A.; Hecht, S. M. *J. Biol. Chem.* **1994**, *269*, 10899.

(12) (a) Wu, J. C.; Kozarich, J. W.; Stubbe, J. *Biochemistry* **1985**, *24*, 7562. (b) Kozarich, J. W.; Worth, L., Jr.; Frank, B. L.; Christner, D. F.; Vanderwall, D. E.; Stubbe, J. *Science* **1989**, *245*, 1396.

(13) Van Atta, R. B.; Long, E. C.; Hecht, S. M.; van der Marel, G. A.; van Boom, J. H. *J. Am. Chem. Soc.* **1989**, *111*, 2722.

(14) Manderville, R. A.; Ellena, J. F.; Hecht, S. M. *J. Am. Chem. Soc.* **1994**, *116*, 10851.

(15) Hénichart, J.-P.; Bernier, J.-L.; Helbecque, N.; Houssin, R. *Nucleic Acids Res.* **1985**, *13*, 6703.

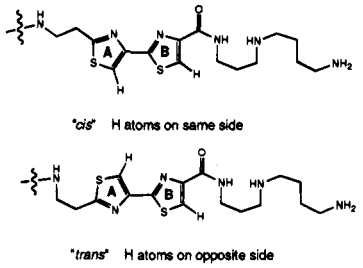

Figure 2. Two possible planar orientations of the bithiazole ring system.

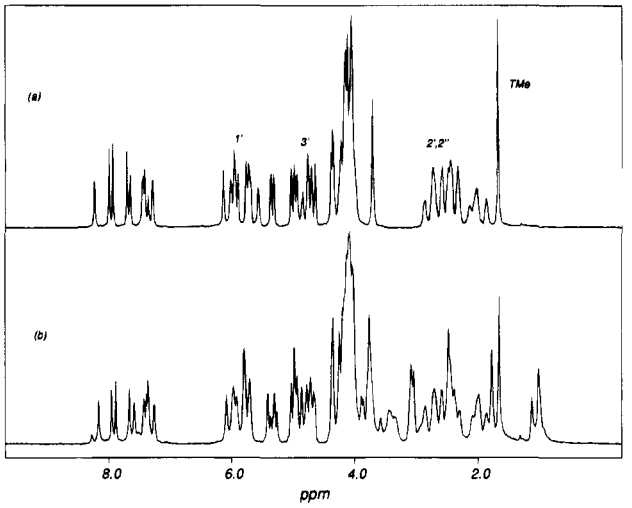

Figure 3. ^{1}H NMR spectra of (a) d(CGCTAGCG)$_2$ and (b) the 1:1 complex of Zn(II)·BLM A$_5$–d(CGCTAGCG)$_2$ in D_2O at 35 °C. Samples contained 4.2 mM DNA duplex, pH 7.0, with 20 mM NaCl. Assignments of the DNA deoxyribose H1′,H3′ and H2′,2″ and the thymidine$_4$ methyl group are indicated in spectrum (a).

DNA structures shows that Zn(II)·BLM binding is accompanied by widening of the minor groove, a decrease in the base-pair helical twist, and an increase in roll angle at the bithiazole binding site.

Results

^{1}H NMR Assignments. Shown in Figure 3 are one-dimensional ^{1}H NMR spectra in D_2O of d(CGCTAGCG)$_2$, both in the absence and presence of 1 equiv of Zn(II)·BLM A$_5$. The broadening and shifting of the DNA resonances demonstrates binding of the drug. This is particularly apparent for the H1′ protons of the deoxyribose sugars, which lie in the minor groove. In contrast, the H3′ protons in the major groove show very little change upon admixture of Zn(II)·BLM A$_5$. These features are consistent with Zn(II)·BLM binding in the minor groove of the octanucleotide. Also evident is the fact that the strands of the self-complementary oligonucleotide remain equivalent, indicating that Zn(II)·BLM A$_5$ is in fast exchange between the symmetry-related DNA binding sites.

Figure 4 shows the aromatic region in D_2O (7.1–8.4 ppm) of Zn(II)·BLM A$_5$, both free and in the presence of 1 equiv of the d(CGCTAGCG)$_2$. For the free Zn(II)·BLM A$_5$ complex, a total of four resonances, belonging to the bithiazole and β-hydroxyhistidine residues, are present. At 35 °C, the bithiazole H5′ (Bit 5′) and β-hydroxyhistidine H2 (His 2) peaks overlap at ~8.06 ppm. Upon addition of the DNA oligonucleotide, the bithiazole 5 and 5′ protons broaden considerably and shift upfield from 8.21 and 8.04 to 8.03 and 7.52 ppm, respectively. Compared to the free state, this represents an upfield shift of 0.18 ppm for Bit 5 of the B-ring and 0.52 ppm for Bit 5′ of the A-ring. These shifts are consistent with a

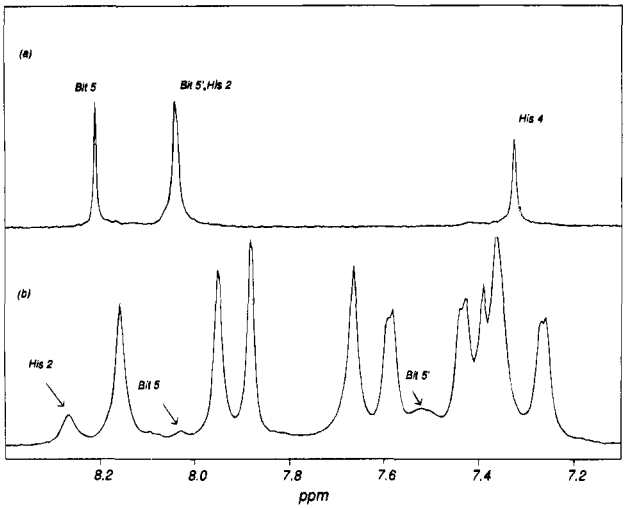

Figure 4. Aromatic region (7.1–8.4 ppm) of ^{1}H NMR spectra of (a) Zn(II)·BLM A$_5$ and (b) the 1:1 complex of Zn(II)·BLM A$_5$–d(CGCTAGCG)$_2$ in D_2O at 35 °C. Assignments of the β-hydroxyhistidine protons (His 2, His 4) and bithiazole protons (Bit 5, Bit 5′) are indicated.

structure in which the bithiazole ring system partially stacks between the DNA base pairs. Further, the data indicate preferential shielding of Bit 5′ of the A-ring.[10a,15] The extensive line broadening could indicate that BLM is binding to the octanucleotide in multiple conformations, at multiple sites, or both. Notably in this regard, the relatively high temperatures (35 °C) utilized in this study were required to observe the bithiazole resonances. In fact, the chemical shifts of these resonances are highly temperature dependent;[10a] at lower temperatures (e.g., 25 °C) these peaks are not observed.

Also apparent from Figure 4 is broadening and downfield shifting (+0.16 ppm) of the β-hydroxyhistidine H2 (His 2) resonance. The histidine ring of BLM participates in metal ion coordination.[8] Broadening and shifting of this resonance suggests binding to the DNA and lends support to the idea that the metal binding domain of BLM participates in DNA binding.[7] The downfield shift of His 2 is consistent with a groove binding mode, as the His 2 proton interacts with the edges of the DNA base pairs.[16] Assignment of the His 4 resonance was achieved from inspection of the DQF-COSY spectrum of the Zn(II)·BLM A$_5$–d(CGCTAGCG)$_2$ complex, where a weak cross peak between His 2 and His 4 is observable. The His 4 peak similarly shifts downfield upon DNA binding but to a lesser extent (+0.09 ppm).

The imino proton region of the octanucleotide was examined in spectra acquired in H_2O (supplementary material, Figure 1). At 35 °C, the free octanucleotide shows three imino proton resonances. The terminal guanosine$_8$ NH peak is not visible due to exchange with solvent.

The addition of Zn(II)·BLM A$_5$ resulted in broadening and upfield shifting (−0.1 ppm) of the thymidine$_4$ and guanosine$_2$ NH protons, while the chemical shift of the guanosine$_6$ NH proton remains fairly constant. Upfield shifting of the DNA base-paired imino protons upon ligand binding is consistent with a binding mode involving intercalation.[17] In the present system, the chemical shift changes of the DNA imino protons are small (−0.1 ppm), which may simply reflect differences in base stacking or changes in nucleic acid conformation.[16] However, coupled with the broadening and upfield shifting of the bithiazole resonances, these changes in the DNA imino protons

(16) Wilson, W. D.; Li, Y.; Veal, J. M. *Adv. DNA Sequence Specific Agents* **1992**, *1*, 89.

Table 1. ^{1}H NMR Chemical Shifts (ppm) of Zn·BLM A_5, Zn·BLM A_2 and with Equimolar d(CGCTAGCG)$_2$ (+DNA) at 35 °C, 20 mM NaCl, pH 7.0

residue	Zn(II)·BLM A_5	+DNA	Δδ	Zn(II)·BLM A_2	+DNA	Δδ
Ala α	3.79	3.88	+0.09	3.77	3.82	+0.05
Ala β	2.54	2.48	−0.06	2.54	2.51	−0.03
Ala β′	3.42	3.36	−0.06	3.40	3.39	−0.01
Ala NH[a]	4.35	n.d.[b]		4.35	n.d.	
Pro α	2.93	2.87	−0.06	2.92	2.88	−0.04
Pro α′	3.33	3.44	+0.11	3.33	3.40	+0.07
Pro β	4.59	4.83	+0.24	4.60	4.72	+0.12
Pyr Me	2.44	2.49	+0.05	2.45	2.48	+0.03
Pyr NH2	7.02	7.08	+0.06	7.02	n.d.	
His α	4.91	4.93	+0.02	4.87	4.92	+0.05
His β	5.25	5.27	+0.02	5.23	5.24	+0.01
His 2	8.08	8.24	+0.16	8.08	8.18	+0.10
His 4	7.31	7.40	+0.09	7.35	7.38	+0.03
Val α	1.97	1.84	−0.13	1.95	1.91	−0.04
Val β	3.47	3.62	+0.15	3.40	3.50	+0.10
Val γ	3.68	3.70	+0.02	3.65	3.68	+0.03
Val αMe	1.01	1.04	+0.03	0.98	0.99	+0.01
Val γMe	0.98	1.04	+0.06	0.93	0.99	+0.06
Val NH	7.48	7.44	−0.04	7.48	n.d.	
Thr α	4.16	4.26	+0.10	4.17	4.21	+0.04
Thr β	4.06	4.16	+0.10	4.04	4.10	+0.06
Thr Me	1.08	1.14	+0.06	1.05	1.08	+0.03
Thr NH	7.91	7.67	−0.24	7.91	n.d.	
Bit α	3.23	3.05	−0.18	3.25	3.04	−0.21
Bit β	3.61	3.48	−0.13	3.61	3.49	−0.12
Bit 5	8.21	8.03	−0.18	8.21	8.02	−0.19
Bit 5′	8.04	7.52	−0.52	8.04	7.52	−0.52
Bit NH	8.30	8.28	−0.02	8.30	n.d.	
Gul 1	5.36	5.36		5.33	5.35	+0.02
Gul 2	4.13	4.13		4.12	4.14	+0.02
Gul 3	4.09	4.10	+0.01	4.07	4.10	+0.03
Gul 4	3.78	3.75	−0.03	3.77	3.77	
Gul 5	3.90	3.89	−0.01	3.89	3.88	−0.01
Gul 6,6′	3.67, 3.77	3.76, 3.79	+0.09, +0.02	3.67, 3.75	3.70, 3.75	+0.03
Man 1	4.95	4.96	+0.01	4.94	4.96	+0.02
Man 2	4.14	4.08	−0.06	4.10	4.12	+0.02
Man 3	4.09	4.10	−0.01	4.09	4.08	−0.01
Man 4	3.75	3.76	+0.01	3.75	3.74	−0.01
Man 5	3.77	3.76	−0.01	3.75	3.75	
Man 6,6′	3.85, 4.02	3.88, 4.02	+0.03	3.85, 4.00	3.85, 4.02	+0.02
RNH	8.90	8.58	−0.32	8.90	n.d.	
Sul α				3.40	3.40	
Sul β				2.17	2.12	−0.05
Sul γ				3.62	3.51	−0.11
Sul Me_2^+				2.89	2.92	+0.03
Sp 1	3.56	3.33, 3.42	−0.23, −0.14			
Sp 2	2.05	1.97	−0.08			
Sp 3	3.14	3.10	−0.04			
Sp 4	3.10	3.08	−0.02			
Sp 5	1.77	1.78	+0.01			
Sp 6	1.76	1.78	+0.02			
Sp 7	3.04	3.04				

[a] Assignments of exchangeable protons determined in 9:1 H_2O-D_2O at 15 °C for free Zn·BLM; those in the Zn·BLM-DNA complex at 35 °C. [b] n.d.; not determined.

lend support to the existence of stacking interactions between the bithiazole and DNA base pairs.

Assignments of the individual DNA imino protons in the Zn(II)·BLM A_5−d(CGCTAGCG)$_2$ complex were established by means of one-dimensional NOE experiments. These studies also permitted unambiguous assignment of the base-paired adenosine$_5$ H2 proton, as it shows a strong NOE to the thymidine$_4$ imino proton (data not shown). Other proton chemical shifts were established by means of DQF-COSY and NOESY experiments carried out in D_2O and H_2O. Previous assignments for all the protons and carbon chemical shifts of the Zn(II)·BLM A_2 complex derived from $^1H-^{13}C$ NMR methods, particularly for the disaccharide portion of Zn(II)·BLM, provided valuable guidance for the assignments made in this study.[18]

Table 1 contains the ^{1}H shifts for Zn(II)·BLM A_5 and Zn(II)·BLM A_2, both free and when bound to d(CGCTAGCG)$_2$ at 35 °C, in solutions containing 20 mM NaCl. The free Zn(II)·BLM molecules were also examined at 15 °C, and chemical shifts for exchangeable protons, obtained in 9:1 H_2O-D_2O, are given at this temperature. The Zn(II)·BLM A_2−d(CGCTAGCG)$_2$ complex was examined in D_2O at 35 °C. For the Zn(II)·BLM A_5−d(CGCTAGCG)$_2$ complex, spectra were acquired in both D_2O and 9:1 H_2O-D_2O. For spectra acquired in 90% H_2O, the relatively high temperatures (35 °C) made it difficult to assign all the exchangeable protons of the drug−

(17) Feigon, J.; Denny, W. A.; Leupin, W.; Kearns, D. R. *J. Med. Chem.* **1984**, *27*, 450.
(18) Akkerman, M. A. J.; Haasnoot, C. A. G.; Hilbers, C. W. *Eur. J. Biochem.* **1988**, *173*, 211.

Table 2. ^{1}H NMR Chemical Shifts (ppm) of the DNA Resonances in the Zn(II)·BLM A_5–d(CGCTAGCG)$_2$ Complex at 35 °C, pH 7.0, Containing 20 mM NaCl[a]

	NH	NH_2	H6/H8	H5/H2	H1′	H2′	H2″	H3′	H4′	H5′,5″
C_1			7.57 (−0.7)	5.80 (−0.12)	5.80	2.00	2.44	4.71	4.08	3.74
G_2	12.88 (−0.1)	6.89	7.95		5.91	2.68	2.74	4.98	4.38	4.10, 4.02
C_3		8.30, 6.56	7.43	5.41	5.96	2.09	2.48	4.72 (−0.05)	4.25	4.19
T_4	13.65 (−0.1)		7.37	1.66	5.70 (+0.1)	2.03 (−0.08)	2.40	4.86	4.09	4.06
A_5			8.16 (−0.06)	7.35	5.99	2.71	2.85	5.03	4.34 (−0.08)	4.12, 4.01
G_6	12.78	6.89	7.67		5.72	2.46	2.58	4.93	4.35	4.19
C_7		8.22, 6.41	7.27	5.30	5.77	1.86	2.30	4.77	4.04 (−0.09)	4.14
G_8			7.89		6.09 (−0.07)	2.59	2.37	4.64	4.12	4.01

[a] Values in parentheses represent chemical shift changes from free octamer that are ≥ |0.05| ppm.

DNA complex. Efforts to make ^{1}H assignments at lower temperatures (e.g., 15 °C) were not successful due to extensive line broadening of the resonances.

Inspection of Table 1 reveals some general characteristics. Upfield shifts are observed for protons of the bithiazole (Bit) and cationic R group (Sul for A_2, Sp for A_5) upon DNA binding. For the cationic substituents, the changes in chemical shift ($\Delta\delta$) diminish as the distance from the bithiazole ring increases. For example, the spermidine H1 atoms (Sp 1) shift upfield and become nonequivalent (−0.23, −0.14), while the Sp 3 protons show a small shift (−0.04). Downfield shifts are noted for some protons in the metal binding domain. For the Zn(II)·BLM A_5 system, these include His 2 (+0.16 ppm), His 4 (+0.09 ppm), Pro α′ (+0.11 ppm), Pro β (+0.24 ppm), and Ala α (+0.09 ppm). Taken together, these chemical shift changes are consistent with (partial) intercalation of the bithiazole coupled with minor groove binding by the metal binding domain of BLM. The ^{1}H chemical shifts of the sugar moieties (Gul, Man) of BLM show very little change upon DNA binding, a feature consistent with the interpretation that these groups do not interact strongly with the helix. Also apparent are the greater chemical shift changes ($\Delta\delta$) for the Zn(II)·BLM A_5 system relative to the Zn(II)·BLM A_2 system. This observation is in keeping with the greater potency of BLM A_5 as a DNA and RNA damaging agent,[19] which presumably parallel enhanced binding by this congener.

Table 2 shows the ^{1}H chemical shifts of the DNA resonances in the Zn(II)·BLM A_5 - d(CGCTAGCG)$_2$ complex. Chemical shift values for the octanucleotide in the Zn(II)·BLM A_2–d(CGCTAGCG)$_2$ complex were essentially the same as the values given in Table 2. Compared to the free octanucleotide, only small changes were noted; values in parentheses represent chemical shift changes of free versus bound octanucleotide that were ≥ |0.05| ppm. Generally, upfield shifts are observed, especially for the aromatic protons of cytidine$_1$. These shifts may reflect improved base stacking interactions upon BLM binding; these would be consistent with the known tendency of BLM to stabilize the B-form helix[20] and increase T_m.[15,21] An exception to this trend is the relatively large downfield shift for the thymidine$_4$ H1′ proton (+0.1 ppm). A possible reason for this shift could relate to its position near the edges of the bithiazole rings of BLM, although conformational differences in the bound DNA structure may also account for this shift.

DNA Structure. The conformations of the octanucleotide, both free and bound to Zn(II)·BLM, were estimated using the procedure described by Kim et al.[22] and more recently by Schweitzer and co-workers.[23] This procedure relies on an estimation of the deoxyribose coupling constants to apply constraints on the pseudorotation angle (P)[24] of the sugar ring for each nucleotide. Additional constraints on P can be obtained from NOESY-determined distances, especially the H1′–H4′ distance which is highly dependent on the sugar pucker.[22]

The J coupling measurements from the E-COSY type spectrum[25] of the free octanucleotide and the Zn(II)·BLM–DNA complex (supplementary material, Table 1) indicate that $J_{1'-2'}$ is greater than $J_{1'-2''}$ for every residue, an observation that limits all of the deoxyribose pseudorotation angles to 90–190°.[23] In the H3′–H2′2″ region of the DQF-COSY spectrum of the Zn(II)·BLM A_5–d(CGCTAGCG)$_2$ complex (Figure 5), only the terminal guanosine$_8$ residue shows a relatively strong H2″-H3′ cross peak. As shown in Figure 5, the cytidine$_7$ residue also shows a H2″-H3′ cross peak, but it is barely detectable. These characteristics were also apparent for the free octanucleotide and indicate that the octanucleotide retains its B-form conformation upon Zn(II)·BLM binding.

While other coupling constants ($J_{2''-3'}$ and $J_{3'-4'}$) of the deoxyribose sugars are difficult to determine accurately due to passive couplings,[25] the intensity of the cross peaks are related to the magnitude of the active J couplings.[23] Inspection of the H3′–H4′ region (supplementary material, Figure 2) of the DQF-COSY spectrum for the free and bound octanucleotide shows cross peaks for every residue, although those of guanosine$_2$ and adenosine$_5$ are particularly weak. The fact that guanosine$_2$ and adenosine$_5$ have weak H3′–H4′ couplings, in combination with the absence of H2″–H3′ couplings, constrains P for these residues to the range (140–162°) including twisted forms of C2′-endo, where C2′-endo is defined as P = 162°. All other residues have medium to strong H3′-H4′ cross peaks. Thus, for residues C_1, C_3, T_4, G_6, and C_7, which show nonexistent or extremely weak H2″–H3′ cross peaks, P was constrained to a wider range (P = 120–162°) that includes both C2′-endo and C1′-exo along with twisted intermediates, where C1′-exo is defined as P = 126°. The terminal guanosine$_8$ residue P was constrained to a range (P = 72–100°) that included the O4′-endo sugar pucker (P = 90°), since it exhibits an H2″–H3′

(19) Holmes, C. E.; Hecht, S. M., unpublished observations.
(20) Hertzberg, R. P.; Caranfa, M. J.; Hecht, S. M. *Biochemistry* **1988**, *27*, 3164.
(21) (a) Povirk, L. F.; Hogan, M.; Dattagupta, N. *Biochemistry* **1979**, *18*, 96. (b) Fisher, L. M.; Kuroda, R.; Sakai, T. T. *Biochemistry* **1985**, *24*, 3199.
(22) Kim, S.-G.; Lin, L.-J.; Reid, B. R. *Biochemistry* **1992**, *31*, 3564.
(23) Schweitzer, B. I.; Mikita, T.; Kellogg, G. W.; Gardner, K. H.; Beardsley, G. P. *Biochemistry* **1994**, *33*, 11460.
(24) (a) Haasnoot, C. A. G.; de Leeuw, F. A. A. M.; Altona, C. *Tetrahedron* **1980**, *36*, 2783. (b) Van Wijk, J.; Huckriede, B. D.; Ippel, J. H.; Altona, C. *Methods Enzymol.* **1992**, *211*, 286.
(25) Bax, A.; Lerner, L. *J. Magn. Reson.* **1988**, *79*, 429.

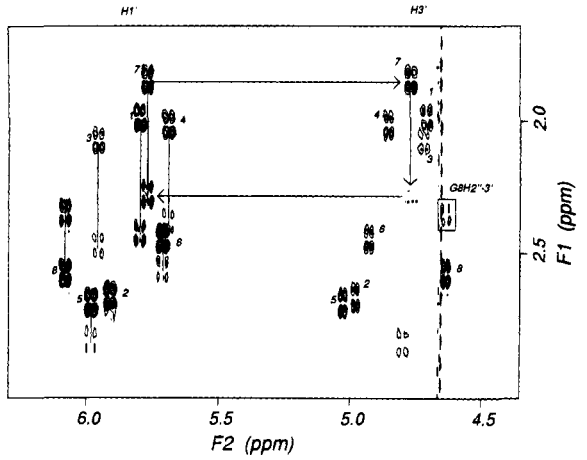

Figure 5. Assignment of 2′,2″, and 3′ protons of the deoxyribose sugars in the Zn(II)·BLM A_5–d(CGCTAGCG)$_2$ complex. The DQF-COSY ^{1}H NMR spectrum was taken in D_2O at 35 °C. Cross peaks between 1′-2′ and 1′-2″ protons are indicated by residue number. Except for the 3′ terminal guanosine$_8$ residue, 2′ protons resonate upfield relative to the 2″ proton of the same residue. The arrows illustrate the extension of the assignment from 2′,2″ protons to the 3′ proton for residue cytidine$_7$. Cross peaks between 2′ and 3′ are noted by base residue number.

cross peak and a strong H3′–H4′ cross peak.[23] These values were converted into ranges for the individual sugar torsion angles, ν, using the relationship $\nu_j = T_m \cos[P + 144(j - 2)]$, where T_m is 35° and j is 0–4.[24] These torsion angles were included in the restrained molecular dynamics calculations.

BLM–BLM and BLM–DNA NOEs. The structures of the free Zn(II)·BLM A_2 and Zn(II)·BLM A_5 complexes were examined by 2D NMR at 15 °C in D_2O and in 9:1 H_2O–D_2O, containing 20 mM NaCl, pH 7.0. As observed previously,[18] the NOESY spectrum (τ_{mix} = 300 ms) displays nonvicinal intramolecular NOEs that occur between protons of the metal binding domain and protons on the methyl valerate residue. No NOEs are observed from protons of the metal binding domain to those from the threonine and bithiazole residues, a result which suggests that the free Zn(II)·BLM structures are either extended, highly flexible, or both.[18]

Upon DNA binding, an intramolecular NOE between H2 of the β-hydroxyhistidine group (His 2) and the threonine methyl (Thr Me) was noted both for Zn(II)·BLM A_5 and Zn(II)·BLM A_2. This NOE has also been detected for the free green Co(III)·BLM A_2 complex,[26] which has been shown to adopt a folded conformation. Further evidence for folding of the BLM structure is derived from the finding of intermolecular NOEs to the DNA that necessitate the close proximity of the functional domains of BLM.

At 35 °C, we were able to detect eight intermolecular BLM-DNA NOEs for the Zn(II)·BLM A_5–d(CGCTAGCG)$_2$ complex. These were used to define the alignment of the drug relative to the helix (Figure 6). The bithiazole H5 proton (Bit 5) of the B-ring and the H3 atoms of the cationic spermidine C-terminal substituent showed contacts to adenosine$_5$ H2 in the minor groove. The bithiazole H5′ proton (Bit 5′) shows intermolecular NOEs with thymidine$_4$ H6 and cytidine$_3$ H6, which are located in the major groove. These major groove contacts for Bit 5′ of the bithiazole A-ring are consistent with its preferential shielding and indicates that the A-ring is stacking with thymidine$_4$ and cytidine$_3$. These contacts are also consistent with the observed broadening and upfield shifting of the thymidine$_4$ imino proton. For the B-ring of the bithiazole and spermidine group, the contact with adenosine$_5$ H2 indicates that these protons lie more in the minor groove,[17] which is consistent with the smaller amount of shielding for Bit 5. These contacts and the degree of shielding appear to indicate that the bithiazole is partially stacked between the A_5G_6 and the base-paired C_3T_4 step of the octamer.

Evidence against a classical intercalation binding mode derives from the finding that binding of Zn(II)·BLM to the octanucleotide does not disrupt the sequential NOE assignments. Figure 7 shows an expansion of the aromatic region of the NOESY spectrum obtained at 35 °C for the Zn(II)·BLM A_5–d(CGCTAGCG)$_2$ complex. The intermolecular NOEs between the DNA and the aromatic bithiazole protons referred to above are labeled. The sequential NOE assignments between the base and H1′ protons of the octamer are also shown. The fact that binding of BLM does not disrupt the sequential NOE assignments of the octanucleotide clearly rules out a classical intercalation mechanism, since intercalators disrupt the DNA sequential interresidue NOEs by causing helical unwinding and elongation that increases the distance between base steps to ≥5 Å.[27]

From examination of the Zn(II)·BLM A_5 and Zn(II)·BLM A_2 complexes with d(CGCTAGCG)$_2$, strong supportive evidence for the assignments of the intermolecular BLM–DNA NOEs (Figure 6) was obtained. The NOESY spectra of the two complexes were quite similar, although the H8/H6–H2′,2″ region was better resolved in the Zn(II)·BLM A_2 complex. Figure 8 shows an expansion of the H8/H6–H2′,2″ region of the NOESY spectrum of the Zn(II)·BLM A_2–d(CGCTAGCG)$_2$ complex. The sequential connectivities are clearly visible, as is a weak NOE between Bit 5′ and thymidine$_4$ Me. In the aromatic region of the spectrum, a weak Bit 5′-cytidine$_3$ H5 NOE was also noted (not shown). These observations strongly support a model in which the bithiazole A-ring is positioned between the C_3T_4 base step. Deviations in the DNA structure that reflect this binding mode for Zn(II)·BLM can be derived from inspection of the H8/H6–H1′ region of the NOESY spectrum for the Zn(II)·BLM A_5–d(CGCTAGCG)$_2$ complex (Figure 7). The T_4 H6–C_3 H1′ and A_5 H8–T_4 H1′ NOEs are particularly weak, while the G_6 H8–A_5 H1′ NOE is quite strong. However, in the H8/H6–H2′2″ region the NOEs are quite strong (Figure 8). These results indicate a change in the DNA structure upon BLM binding. Unfortunately, in the Zn(II)·BLM A_2–d(CGCTAGCG)$_2$ system no NOE contact between the helix and the cationic C-substituent was detected.

The preferred orientation of the metal binding domain with the cytidine$_7$ residue is based on the observation of intermolecular NOEs between protons of the methyl valerate and β-hydroxyhistidine residues with minor groove protons of cytidine$_7$.[14] The gulose H6,6′ atoms also show a weak cross peak to thymidine$_4$ H3′. This cross peak positions the gulose moiety near the strand opposite the cytidine$_7$ cleavage site.

Support for some of the BLM–DNA NOE assignments was obtained from a study of the Zn(II)·BLM A_5–d(CGCTAGCG)$_2$ system under high salt conditions (200 mM NaCl, data not shown), which was carried out in an effort to examine the spectrum at lower temperature (−5 °C). The bithiazole ring system remains bound to the DNA, as these resonances are still exchange-broadened. Further, the NOEs between DNA and the bithiazole region remained intact. Interestingly, at high salt, protons of the metal binding domain shifted back to the positions observed for Zn(II)·BLM A_5 in the free state. Further, the

(26) Xu, R. X.; Nettesheim, D.; Otvos, J. D.; Petering, D. H. *Biochemistry* **1994**, *33*, 907.

(27) (a) Liu, X. L.; Chen, H.; Patel, D. J. *J. Biomol. NMR* **1991**, *1*, 323. (b) David, S. S.; Barton, J. K. *J. Am. Chem. Soc.* **1993**, *115*, 2984.

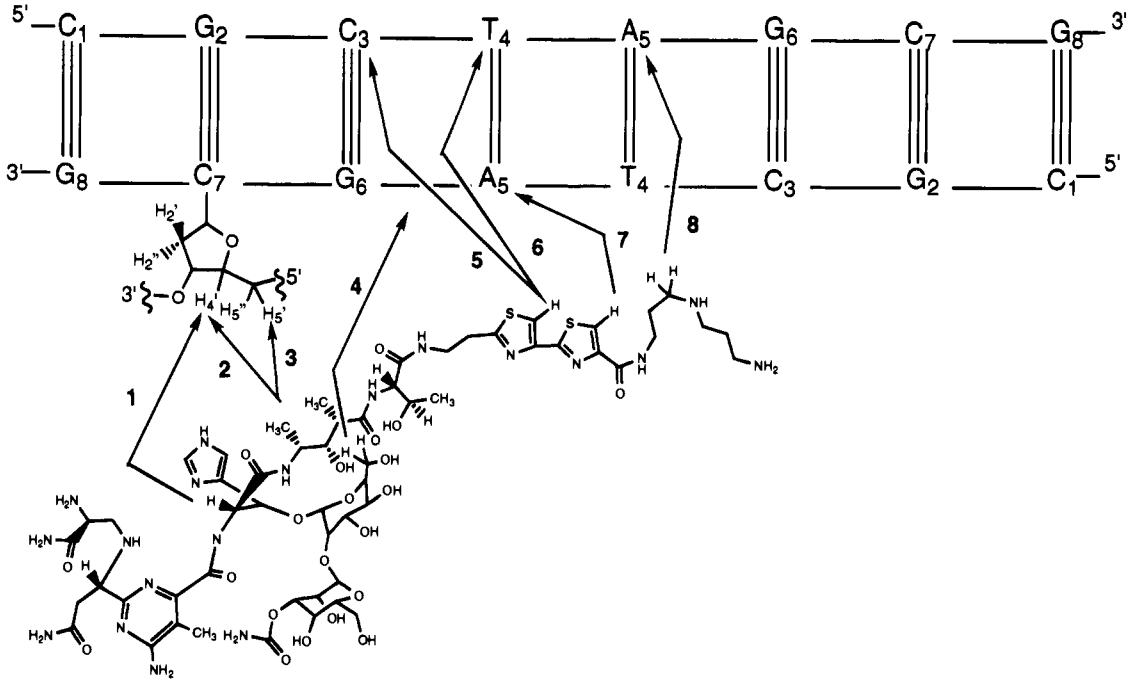

Figure 6. Schematic diagram showing the eight intermolecular NOEs between Zn(II)·BLM A_5 and d(CGCTAGCG)$_2$. With the exception of NOE 8, the analogous NOEs were observed for the Zn(II)·BLM A_2—d(CGCTAGCG)$_2$ complex. Assignments: 1, C_7 H4′ - His Hα; 2, C_7 H4′ - Val Me; 3, C_7 H5′,5″- Val Me; 4, T_4 H3′ - Gul H6, H6′; 5, C_3 H6 - Bit 5′; 6, T_4 H6 - Bit 5′; 7, A_5 H2 - Bit 5; 8, A_5 H2 - Sp 3. It was not possible to distinguish between the two CH_3 groups of the methyl valerate moiety.

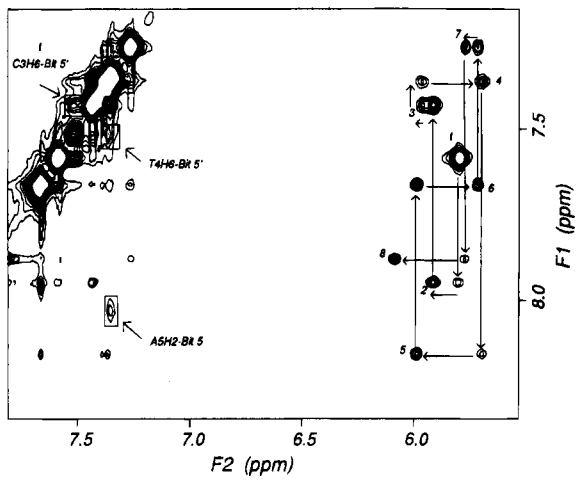

Figure 7. Expanded NOESY ^{1}H NMR spectrum of the Zn(II)·BLM A_5—d(CGCTAGCG)$_2$ complex in D_2O at 35 °C, τ_{mix} = 300 ms. Sequential aromatic (H8/H6) to C1′H connectivities for the octanucleotide are denoted by arrows and residue numbers are indicated. Intermolecular DNA—BLM cross peaks from the aromatic bithiazole protons (Bit 5, Bit 5′) to adenosine$_5$ H2, thymidine$_4$ H6, and cytidine$_3$ H6 are also indicated.

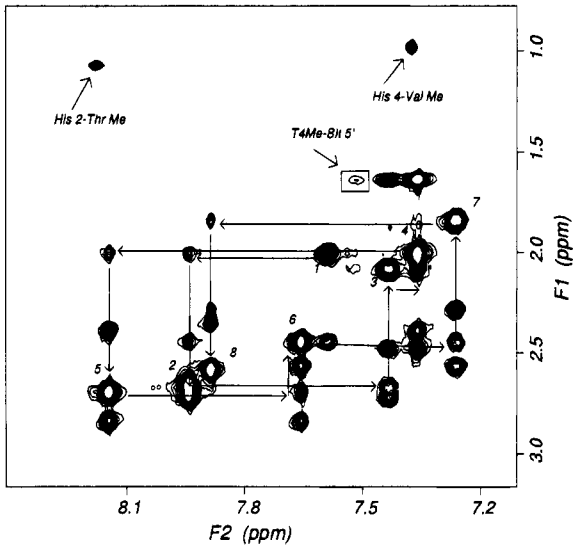

Figure 8. Expanded NOESY ^{1}H NMR spectrum of the Zn(II)·BLM A_2—d(CGCTAGCG)$_2$ complex in D_2O at 35 °C, τ_{mix} = 300 ms. Sequential aromatic (H8/H6) to C2′H connectivities for the octanucleotide are denoted by arrows. Intramolecular BLM - BLM cross peaks from aromatic protons of the β-hydroxyhistidine residue (His 2, His 4) to the threonine methyl group (Thr Me) and methyl valerate methyl group (Val Me) are shown. A weak intermolecular BLM—DNA cross peak between the thymidine$_4$ methyl group (T_4Me) and bithiazole H5′ (Bit 5′) is also indicated.

previously observed NOEs between the metal binding domain of BLM and the DNA oligomer disappeared. Such results are consistent with the ionic and nonionic components of DNA binding by BLM described previously.[9,10a,28]

The intramolecular BLM—BLM NOEs and intermolecular BLM—DNA NOEs that we have been able to assign for the Zn(II)·BLM A_5—d(CGCTAGCG)$_2$ complex are listed in Table 3. These NOEs were converted into distance ranges and were used as restraints to guide the molecular dynamics calculations.

Molecular Modeling. Modeling of the Zn(II)·BLM A_5—d(CGCTAGCG)$_2$ complex was carried out using the Insight II/Discover program. To model the BLM—metal ion interaction, five-coordinate heme parameters within Insight II were utilized. The metal ion was attached to the secondary amine of Ala, ring nitrogen of Pyr, amide nitrogen and ring nitrogen of His, and carbamoyl nitrogen of Man (Figure 1). The appropriateness of the use of the heme parameters to model the Zn(II)·BLM complex is supported by the following: (i) Coulombic interactions, which diminish as $1/r$, are likely to play a dominant role in the binding energy. Thus, at considerable distances the energy of interaction between the metal binding domain and DNA is not negligible. This makes the charge of the metal

(28) Booth, T. E.; Sakai, T. T.; Glickson, J. D. *Biochemistry* **1983**, *22*, 4211. It may be noted, however, that certain known groove binders undergo upfield shifting of their aromatic protons upon binding to DNA. See, for example, ref 16 and the following: Blaskó, A.; Browne, K. A.; Bruice, T. C. *J. Am. Chem. Soc.* **1994**, *116*, 3726.

Table 3. Nonvicinal Intramolecular BLM–BLM NOEs and Intermolecular BLM–DNA NOEs in Zn(II)·BLM A_5–d(CGCTAGCG)$_2$

intramolecular BLM–BLM NOEs			intermolecular BLM–DNA NOEs	
His 2-Thr Me	His β-Gul 1	Man 1-Man 5	C_7 H4′-His α	T_4 H6-Bit 5′
His 4-Val Me	His β-Gul 5	Sp 1-Sp 3	C_7 H4′-Val Me	C_3 H6-Bit 5′
His 4-Gul 5	His β-Gul 2	Man 3-Ala β,β'	C_7 H5′,5″-Val Me	
His 4-Gul 1	His β-Val Me	Val NH-Val β	T_4 H3′-Gul 6,6′	
His 4-His β	Gul 1-Man 5	Val NH-Val α	A_5 H2-Bit 5	
His β-Man 5	Gul 1-Gul 5	Thr NH-Thr β	A_5 H2-Sp 3	

binding domain a more critical factor than its exact structure. (ii) The five BLM metal binding ligands that we have chosen are regarded as the most likely ligands in the Fe(II)·BLM·CO complex.[8b] (iii) NMR studies show that the structure of Zn(II)·BLM does not vary dramatically from that of Fe(II)·BLM·CO.[8b,18] (iv) Resonance Raman studies indicate that the electronic properties of Fe(II)·BLM·CO are similar to those of CO-bound iron porphyrins.[29]

Using the NOE restraints listed in Table 3 to guide the molecular dynamics calculations, a model for the binding of Zn(II)·BLM A_5 to the octanucleotide was determined. Further, given the small number and intensity of the BLM–DNA NOEs detected for this particular system, a distance restraint between the metal ion of BLM and cytidine$_7$ H4′ was used (between 2 and 6 Å); this seemed reasonable as the metal ion must be within a certain distance of the cytidine$_7$ H4′ atom in order to initiate cleavage via H atom abstraction.[9] Listings of DNA–DNA restraints used in the calculations are available as supplementary material (Tables 2 and 3).

Using the molecular modeling procedure described above and in the Experimental Section, ten structures of the Zn(II)·BLM A_5–d(CGCTAGCG)$_2$ complex were generated. The final energies of these complexes fell within a fairly narrow range, and the average pairwise root mean square differences (RMSDs) for heavy atoms of all ten structures was 1.17 ± 0.73 Å. The pairwise RMSDs between structures, and an overlay of five final Zn(II)·BLM A_5–d(CGCTAGCG)$_2$ structures (major groove view) that satisfy the NOE distance restraints to within 0.2 Å are available as supplementary material (Table 4 and Figure 3, respectively). Although the rather large variation between structures is a reflection of the fact that the NMR data does not indicate a unique BLM–DNA structure, some general characteristics in the structures are apparent, and these features are represented by the model presented in Figures 9 and 10.

Figure 9 shows two views (minor groove (top), major groove (bottom)) of a low energy structure that satisfies all the NOE restraints to within 0.2 Å. The bleomycin molecule fits snugly into the minor groove of the helix. The bithiazole ring system lies parallel to the DNA base pairs and partially enters the helix at the A_5G_6 and base-paired C_3T_4 step. To accommodate the bithiazole moiety a bend in the helix is produced. This bend is achieved by means of a positive roll angle (supplementary material, Figure 4) that opens the base pairs toward the minor groove at the A_5-G_6 base step. The net result is a rather poor stacking of the DNA base pairs. The bithiazole ring system is twisted (Figure 9, major groove view) with a dihedral angle on the order of 20°. This twisting appears to complement the roll of the DNA base pairs.[30] The positively charged spermidine C-substituent lies deep in the minor groove at the T_4-A_5 base step and is stabilized by electrostatic interactions.[31] The drug molecule folds back upon itself through a turn at the junction between the threonine and methyl valerate residues.[10g,32] In eight of the ten structures generated, a hydrogen bond between the NH_2 group of guanosine$_6$ and the hydroxyl group of the methyl valerate residue is assigned by Insight II. The metal ion (white ball) is on the order of 4.5 Å from the cytidine$_7$ H4′ atom, whose abstraction initiates DNA degradation.

Figure 10 shows stereodrawings of the model depicted in Figure 9. An illustration of the stacking arrangement of the bithiazole moiety is shown in the bottom drawing. This view shows that the bithiazole A-ring partially overlaps with thymidine$_4$, which is consistent with the NMR observations in that broadening and upfield shifting of the thymidine$_4$ NH proton is caused by BLM binding. The orientation of the bithiazole with respect to the DNA in the present model constitutes a significant deviation from the model proposed by Kuwahara and Sugiura based on equilibrium binding data.[32] In the latter model the bithiazole moiety is also in a "*cis*" orientation (Figure 2), but the ring N atoms are directed into the helix in a minor groove orientation that favors H-bonding with the 2-NH_2 group of guanine.[32] Both models present the drug molecule in a folded conformation.

Discussion

Both minor groove[14,32,33] and (partial) intercalation[15,21] models have been advanced to explain the binding of the C-terminus of BLM to DNA. In general, unfused aromatic ring systems linked by groups or bonds with potential torsional freedom bind to the minor groove of DNA and typically favor AT-rich regions.[34] Fused aromatic ring systems typically bind to DNA via intercalation and tend to be GC specific.[16] The bithiazole moiety of BLM is an unfused aromatic ring system and might, therefore, be expected to bind to DNA by a minor groove binding mechanism. In this regard, it has been suggested that a groove binding orientation would favor hydrogen bonding from a bithiazole ring N to the guanosine NH_2, which could direct the 5′-Gpyr-3′ sequence selectivity of BLM.[21b,32] In fact, the characterized minor groove binding agent distamycin was shown to alter the specificity of DNA cleavage by BLM.[33a,35]

That the sequence selectivity of DNA degradation noted for BLM need not derive from an intercalative mode of binding is suggested strongly by the structurally similar antitumor antibiotic phleomycin, which differs from BLM only in that it contains a

(29) Takahashi, S.; Sam, J. W.; Peisach, J.; Rousseau, D. L. *J. Am. Chem. Soc.* **1994**, *116*, 4408.

(30) (a) Wilson, W. D.; Strekowski, L.; Tanious, F. A.; Watson, R. A.; Mokrosz, J. L.; Strekowska, A.; Webster, G. D.; Neidle, S. *J. Am. Chem. Soc.* **1988**, *110*, 8292. (b) Strekowski, L.; Mokrosz, J. L.; Wilson, W. D.; Mokrosz, M. J.; Strekowski, A. *Biochemistry* **1992**, *31*, 10802.

(31) (a) Zakrzewska, K.; Pullman, B. *Biopolymers* **1986**, *25*, 375. (b) Schmid, N.; Behr, J.-P. *Biochemistry* **1991**, *30*, 4357.

(32) Kuwahara, J.; Sugiura, Y. *Proc. Natl. Acad. Sci. U.S.A.* **1988**, *85*, 2459.

(33) (a) Sugiura, Y.; Suzuki, T. *J. Biol. Chem.* **1982**, *257*, 10544. (b) Dickerson, R. E. In *Mechanisms of DNA Damage and Repair: Implications for Corcinogenesis and Risk Assessment in Basic Life Sciences*; Sini, M. G., Grossman, L., Eds.; Plenum Press: New York, 1986; p 245. (c) Hiroaki, H.; Nakayama, T.; Ikehara, M.; Uesugi, S. *Chem. Pharm. Bull.* **1991**, *39*, 2780. (d) Tueting, J. L.; Spence, K. L.; Zimmer, M. *J. Chem. Soc., Dalton Trans.* **1994**, 551.

(34) (a) Dervan, P. B. *Science* **1986**, *232*, 464. (b) Lown, J. W. *Chemtracts-Org. Chem.* **1993**, *6*, 205.

(35) Sugiyama, H.; Kilkuskie, R. E.; Hecht, S. M.; van der Marel, G. A.; van Boom, J. H. *J. Am. Chem. Soc.* **1985**, *107*, 7765.

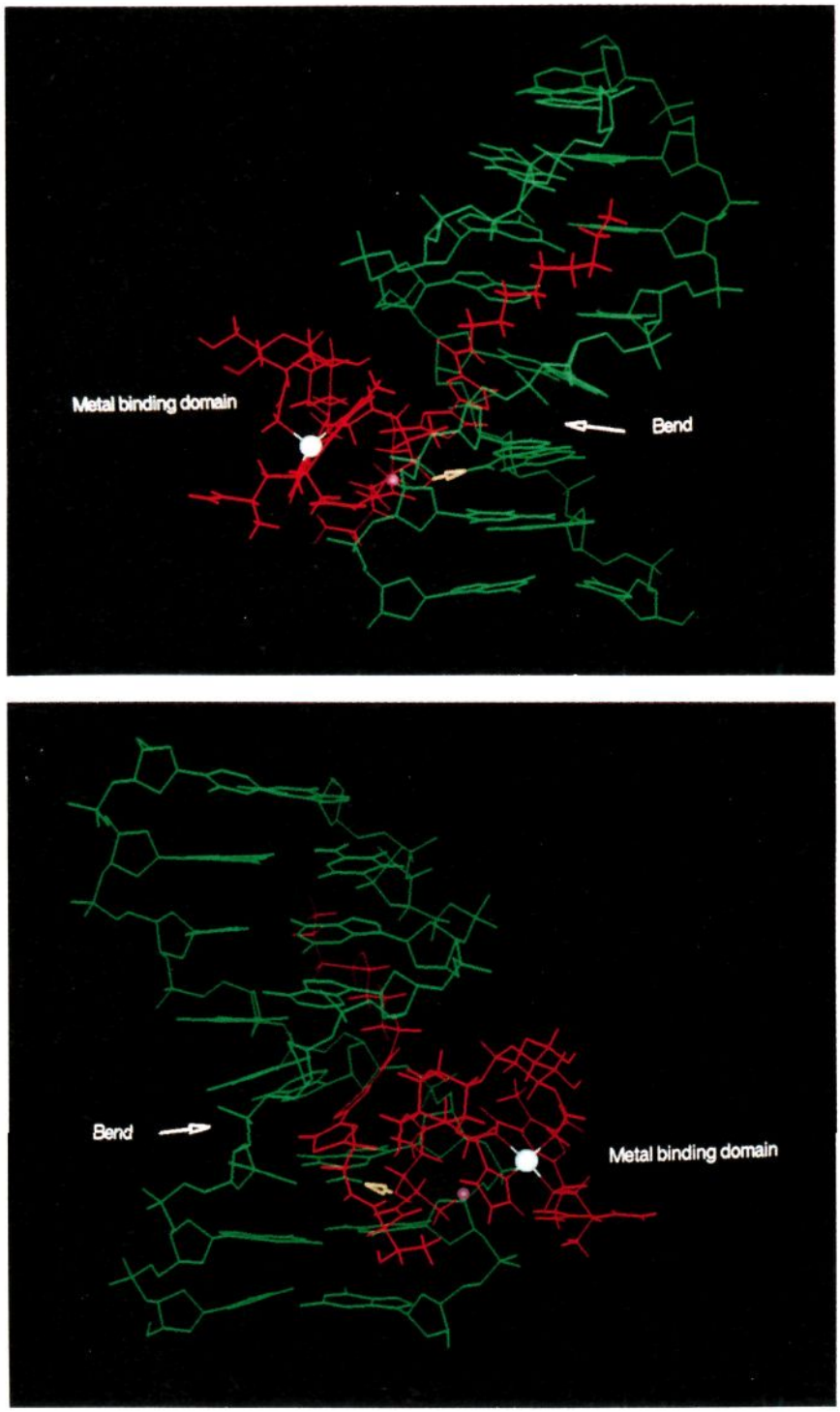

Figure 9. Model of the Zn(II)·BLM A_5−d(CGCTAGCG)$_2$ complex determined by energy minimization and restrained molecular dynamics calculations. For clarity, hydrogen atoms are omitted from the DNA structure (green) but not from the Zn(II)·BLM A_5 model (red). The hydrogen bond between the NH_2 group of guanosine$_6$ and OH of the methyl valerate residue (Val) of BLM is shown as a yellow arrow pointing toward the guanosine$_6$ NH_2 hydrogen atom. The metal ion of BLM (white ball) is 4.5 Å from cytidine$_7$ H4′ (purple ball). (a) Minor groove view (top). Perspective looking into the minor groove of the octanucleotide. The bend in the helix is indicated. (b) Major groove view (bottom). Perspective highlighting the folded BLM molecule and the twist of the bithiazole ring system.

thiazolinylthiazole moiety rather than a bithiazole.[36] The lack of planarity of the thiazolinylthiazole must preclude intercalation;[10d] in fact phleomycin mediates neither helix elongation[10d] nor DNA unwinding.[37] Nonetheless, phleomycin exhibits essentially identical sequence specificity of DNA cleavage as bleomycin.[38]

(36) (a) Takita, T.; Muraoka, Y.; Fujii, A.; Itoh, H.; Maeda, K.; Umezawa, H. *J. Antibiot.* **1972**, *25*, 197. (b) Takita, T.; Muraoka, Y.; Yoshioka, T.; Fujii, A.; Maeda, K.; Umezawa, H. *J. Antibiot.* **1972**, *25*, 755. (c) Takita, T.; Muraoka, Y.; Nakatani, T.; Fujii, A.; Umezawa, Y.; Naganawa, H.; Umezawa, H. *J. Antibiot.* **1978**, *31*, 801. (d) Hamamichi, N.; Hecht, S. M. *J. Am. Chem. Soc.* **1993**, *115*, 12605.

(37) Levy, M. J.; Hecht, S. M. *Biochemistry* **1988**, *27*, 2647.

(38) Kross, J.; Henner, W. D.; Hecht, S. M.; Haseltine, W. A. *Biochemistry* **1982**, *21*, 4310.

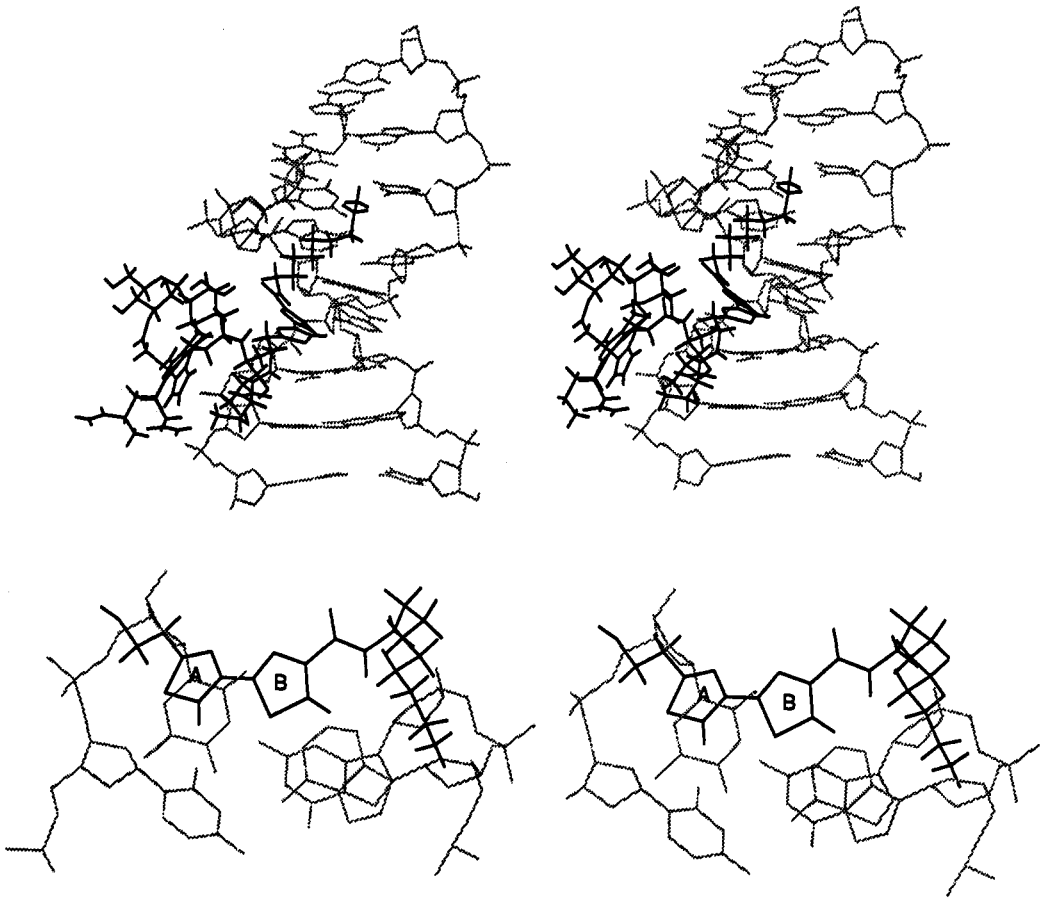

Figure 10. Stereodrawing of the molecular model of the Zn(II)·BLM A_5–d(CGCTAGCG)$_2$ complex obtained by energy minimization and restrained molecular dynamics calculations. Minor groove view (top). For clarity, hydrogen atoms are omitted from the DNA structure shown in grey but not from the Zn(II)·BLM A_5 model in black. View approximately along the global helical axis (bottom). The central T_4–A_5 base pair is shown above the C_3–G_6 base pair. Partial stacking of the bithiazole A-ring with thymidine$_4$ is apparent.

In spite of the foregoing obervations, there are a few lines of evidence that support intercalative binding of BLM to DNA. These include the planar nature of the bithiazole moiety;[39] that BLM effects DNA unwinding[21a,37] and helix elongation suggests that it binds to DNA by intercalation. Also supporting an intercalative binding mode are ^{1}H NMR measurements that indicate the upfield shifting of the two nonexchangeable bithiazole ^{1}H NMR resonances upon DNA binding.[10a,28] A recent study of the binding of a Co·BLM derivative to a GC-rich decanucleotide has also supported an intercalative mechanism.[40]

Other lines of evidence, however, suggest that DNA binding by BLM is not classically intercalative, but represents a partial intercalative binding mode where the bithiazole wedges in between the base pairs which occur at bends in a "kinked" DNA.[28] For example, the results of Hénichart and co-workers[15] show that the motion of a nitroxide spin-label is disrupted when attached to the A-ring of the bithiazole, but not when attached to the B-ring, which is suggestive of a partial intercalative mode where only one of the thiazole rings (the A-ring) is inserted between the base pairs, resulting in a bend at the point of complexation. Evidence that seems to support this type of interaction is derived from studies of helix elongation by BLM, which show that BLM fails to effect viscosity changes in DNA typical of classical intercalation.[10a] Small relative increases in DNA viscosity in a titration with intercalators have been interpreted in terms of DNA bending.[41] Further, DNA unwinding can be mediated by molecules such as steroidal diamines that are clearly not intercalators.[37,42]

In the present study, ^{1}H NMR experiments and restrained molecular dynamics calculations have been utilized to define the DNA binding interaction between Zn(II)·BLM and the octanucleotide d(CGCTAGCG)$_2$. The NMR experiments demonstrate that binding of Zn(II)·BLM to d(CGCTAGCG)$_2$ does not abolish the two-fold symmetry of the self-complementary duplex, and, therefore, Zn(II)·BLM exchange between symmetry-related binding sites is fast on the NMR time scale ($>10^2$ s^{-1}). Further, extensive line broadening of the bithiazole proton resonances suggests that exchange between magnetically inequivalent sites occurs.

Using information derived from the NMR experiments, restrained molecular dynamics calculations were used to assess the structure of the Zn(II)·BLM A_5–d(CGCTAGCT)$_2$ complex. Symmetry was not imposed during the molecular modeling and it is important to note that the structures generated (supplementary material, Figure 3) are in rapid equilibrium with those that involve BLM binding to the mirror image sites. The differences among structures (supplementary material, Table 4 and Figure 3) is consistent with the NMR data, which does not indicate a

(39) The bithiazole moiety of BLM has been shown to exist in a planar conformation in the solid state (Koyama, G.; Nakamura, H.; Muraoka, Y.; Takita, T.; Maeda, K.; Umezawa, H.; Iitaka, Y. *Tetrahedron Lett.* **1968**, 4635). The long wavelength absorption of the bithiazole moiety in solution (λ_{max} 290 nm; Zee-Cheng, K.-Y.; Cheng, C. C. *J. Heterocycl. Chem.* **1970**, *7*, 1439) contrasts sharply with that due to single thiazoles (λ_{max} 238 nm), also arguing for a planar conformation.

(40) Wu, W.; Vanderwall, D. E.; Stubbe, J.; Kozarich, J. W.; Turner, C. J. *J. Am. Chem. Soc.* **1994**, *116*, 10843.

(41) Gabbay, E. J.; Scofield, R. E.; Baxter, C. S. *J. Am. Chem. Soc.* **1973**, *95*, 7850.

(42) (a) Patel, D. J.; Canuel, L. L. *Proc. Natl. Acad. Sci. U.S.A.* **1979**, *76*, 24. (b) Hui, X.; Gresh, N. H.; Pullman, B. *Nucleic Acids Res.* **1989**, *17*, 4177.

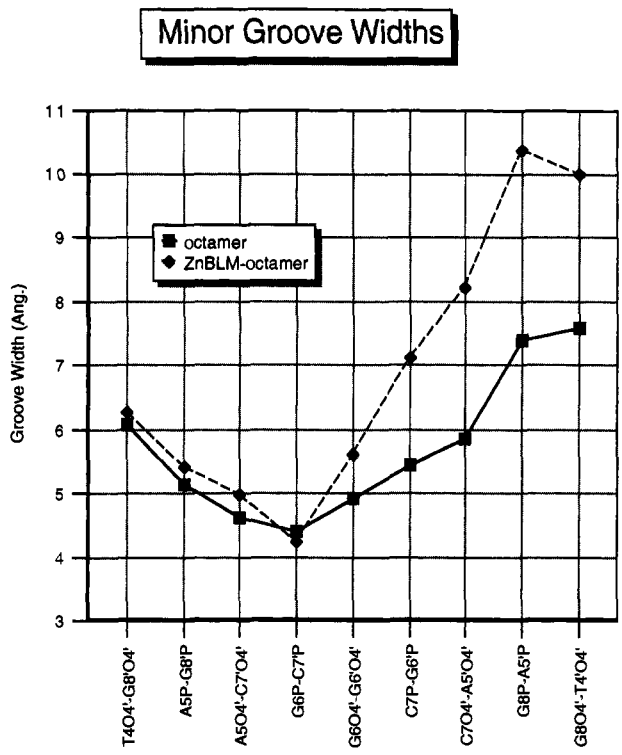

Figure 11. Plot of minor groove widths determined for the free octanucleotide (solid line) versus the Zn(II)·BLM-bound octanucleotide (dotted line). Minor groove widths were measured as the shortest distances between sugar O4′ atoms and phosphate P atoms across the groove. The O4′−O4′ distances are decreased by 2.8 Å, or two oxygen van der Waals radii; those for P by 5.8 Å.

unique structure. In particular, the large line widths of the bithiazole protons are not inconsistent with exchange between (partially) intercalated and minor groove binding locations.

The final structures are also consistent with the possibility of rapid exchange between a partially intercalative bithiazole−DNA interaction and a structurally similar binding arrangement where the plane of the bithiazole rings remains parallel to the base pairs but resides in the minor groove. The "*cis*" orientation (H atoms on same side, Figure 2) permits interaction of the positively charged spermidine C-terminus with the minor groove in the T_4A_5 region and the metal binding domain with the cytidine$_7$ cleavage site. Further, the model (Figures 9 and 10) is in agreement with earlier proposals that posit recognition of the guanosine 2-NH_2 group within the floor of the minor groove;[21b,32] one of these also suggests that BLM binds to DNA as a folded structure.[32]

From the model presented in Figures 9 and 10, measurement of the minor groove widths[43] shows that BLM binding widens the groove (Figure 11). This feature is consistent with the observations that Fe·BLM cleaves DNA preferentially at the sites of bulges[44] and (partially) perturbed duplexes,[4d,45] regardless of DNA sequence, as such sites would necessarily have somewhat wider minor grooves. The model presented also accurately reflects the tendency of BLM to effect DNA unwinding.[15,21,37] Measurement of the global helical twist for the free octanucleotide versus bound (supplementary material, Figure 5) was accomplished using NewHelix.[46] For the free octanucleotide an average helical twist of 38.5° ± 7.3 was determined. This value is in the range expected for a classical B-form conformation.[47] For the bound octanucleotide the average value is lowered to 36.1° ± 7.8. Summation of the changes (free vs bound) in twist angle for the base steps occupied by the drug molecule leads to an unwinding angle of 13°. This value is in good agreement with the literature value of 12° determined experimentally.[21a]

Analysis of the bend in the Zn(II)·BLM−DNA structure (Figures 9 and 10), which occurs at the A_5G_6 base step, shows that the major deviation occurs in the A-T base pair. The net result is a rather large positive roll angle for the A_5G_6 base step. Compared to the free octanucleotide an increase in roll angle of ca 12° is noted (supplementary material, Figure 4). This structural deviation is also reflected in the NOE intensities observed in the NOESY spectra for the Zn·BLM−DNA complex. Measurement of H8/H6−H1′/H2′ distances in the model show that at the bend point the thymidine$_4$ H6−cytidine$_3$ H1′ distance is 5.05 Å, while the base-paired guanosine$_6$ H8−adenosine$_5$ H1′ distance is 3.76 Å. Both steps show short H8/H6−H2′ distances (<3.0 Å). These distances correlate with the NOESY experiments where a particularly weak thymidine$_4$ H6−cytidine$_3$ H1′ NOE and a relatively strong guanosine$_6$ H8−adenosine$_5$ H1′ NOE are observed. Further, both steps show strong sequential H8/H6−H2′ connectivities in the NOESY spectrum (Figure 8).

The effect of this deviation (bend) is a rather poor overlap of the DNA bases at this step. However, the bend in the DNA structure favors partial overlap of the bithiazole ring system (Figure 10, bottom). Inspection of the stacking interaction shows that in addition to π-stacking interactions, edge-to-face stacking interactions are likely to be operative.[48] These types of interactions (edge-to-face) are prevalent for aromatic rings in protein interactions and contribute enthalpic contributions of ca. 2 kcal/mol.[48a]

Other features that emerge from the model (Figures 9 and 10) include the positioning of the bithiazole to the 5′ side of the predominant cytidine$_7$ cleavage site.[35] This orientation is not in agreement with the proposal that BLM binds to DNA on the 3′-side of the cleavage site.[40,44] Clearly this latter proposal cannot obtain for cleavage of d(CGCTAGCG)$_2$ at cytidine$_7$. However, the octanucleotide d(CGCTAGCG)$_2$ is also cleaved at cytidine$_3$ to some extent.[13,35] For cleavage at this site, the bithiazole moiety is positioned in the 3′ direction relative to the site of cleavage. It would appear that cleavage at both cytidine$_7$ and cytidine$_3$ can be facilitated by bithiazole binding at the T_4C_3 step. For example, in the Zn(II)·BLM A_5−d(CGCTAGCG)$_2$ molecule (Figure 9) interstrand cytidine$_3$ H4′ and cytidine$_7$ H4′ atoms are separated by 12.2 Å. Rotation of the metal binding region of the BLM molecule about the threonine residue (the site of the turn that produces a folded structure) positions the metal ion of BLM within 5.4 Å of the cytidine$_3$ H4′ atom. However, in such an orientation, steric contacts are noted between the cytidine$_3$ cleavage site and the disaccharide moiety of Zn(II)·BLM. In this regard, it is interesting to note that cleavage of d(CGCTAGCG)$_2$ by Fe·deglycobleomycin, which lacks the disaccharide moiety, occurs predominantly at cytidine$_3$.

The results of this and other studies suggest strongly that the nature of BLM-DNA interaction is dependent on the DNA sequence. This fact is reflected in the shifting of the bithiazole resonances upon DNA binding. For example, the preferential

(43) Yuan, H.; Quintana, J.; Dickerson, R. E. *Biochemistry* **1992**, *31*, 8009.
(44) Williams, L. D.; Goldberg, I. H. *Biochemistry* **1988**, *27*, 3004.
(45) (a) Gold, B.; Dange, V.; Moore, M. A.; Eastman, A.; van der Marel, G. A.; van Boom, J. H.; Hecht, S. M. *J. Am. Chem. Soc.* **1988**, *110*, 2347. (b) Holmes, C. E.; Hecht, S. M. *J. Biol. Chem.* **1993**, *268*, 25909.
(46) Dickerson, R. E. *J. Biomol. Struct. Dyn.* **1989**, *6*, 627.
(47) Conner, B. N.; Takano, T.; Tanaka, S.; Itakura, K.; Dickerson, R. E. *Nature* **1982**, *295*, 294.
(48) (a) Burley, S. K.; Petsko, G. A. *J. Am. Chem. Soc.* **1986**, *108*, 7995. (b) Askew, B.; Ballester, P.; Buhr, C.; Jeong, K. S.; Jones, S.; Parris, K.; Williams, K.; Rebek, Jr., J. *J. Am. Chem. Soc.* **1989**, *111*, 1082.

upfield shifting of the A-ring bithiazole proton (Bit 5′, 0.52 ppm; Bit 5, 0.18 ppm) observed in the present study is not general for DNA binding by BLM. We have analyzed the interaction of Zn(II)·BLM A_5 with a hexanucleotide $d(ATGCAT)_2$; under fast exchange conditions both bithiazole protons shift upfield to a similar extent (0.50 ppm). Further, when green Co(III)·BLM A_2 binds to the decanucleotide $d(CCAGGCCTGG)_2$ under slow exchange conditions,[40] Bit 5 of the B-ring shifts upfield by 0.9 ppm, while Bit 5′ of the A-ring experiences a 0.61 ppm upfield shift. Taken together, these results suggest that the DNA structure influences the binding mode of BLM.[49]

That the nature of the bithiazole−DNA interaction is sequence dependent is consistent with results for DNA binding of other similar unfused aromatic systems that are in fast exchange.[30] For such molecules it has been suggested that drug−DNA complexes involving minor groove binding and intercalation have comparable energies.[30] Thus, the T_4A_5 region of the octanucleotide $d(CGCTAGCG)_2$ provides electrostatics favorable for a minor groove binding interaction,[34] while the GC-rich sites provide the opportunity for a (partial) intercalative binding mode.[50] Therefore, the model of DNA binding for BLM presented here is in part a reflection of the DNA sequence. At present we are utilizing other metallobleomycins and DNA sequences to define the contribution of each to the formed complexes.

Experimental Section

The octanucleotide ($d(CGCTAGCG)_2$) was prepared on a DNA synthesizer (Biosearch 8600) by phosphoramidite chemistry using standard protocols (15 μmol scale) and purified using HPLC (Varian model 2050) on a reverse phase C_{18} column using a gradient of CH_3CN in 0.1 M ammonium acetate (pH 6.5). Bleomycin A_2 was isolated from blenoxane by elution through a Sephadex column as described[8a,10a] and was purified by HPLC using a reverse phase C_{18} column. Isocratic elution was effected using a gradient of MeOH in 0.1 M ammonium bicarbonate. Bleomycin A_5 was obtained through the courtesy of Dr. Li-Ho Chang, Beijing Medical University.

Sample Preparation. The Zn(II)·BLM A_2−$d(CGCTAGCG)_2$ complex was prepared by dissolving BLM A_2 (3 mM determined spectrophotometrically, ϵ_{292} 14 500 $M^{-1}cm^{-1}$) in 0.4 mL of H_2O. To this solution was added 1 equiv of a $ZnSO_4$ solution (10 μL from a 0.12 M stock solution). The pH of the solution was adjusted to 7.0 using 0.1 M NaOH. The sample was then added to 1 equiv of the octanucleotide (ϵ_{260} 0.812 × 10^5 M^{-1} cm^{-1}). The sample was frozen, lyophilized and rehydrated in 400 μL of 9:1 H_2O−D_2O containing 20 mM NaCl. For spectra acquired in D_2O, the sample was lyophilized three times from 99.9% D_2O and then redissolved in 100% D_2O. The Zn(II)·BLM A_5−$d(CGCTAGCG)_2$ complex (4.2 mM) was prepared in an analogous fashion.

NMR Experiments. One and two-dimensional proton NMR experiments were carried out on a General Electric Omega 500 spectrometer operating at 500.13 MHz using external TSP (3-(trimethylsilyl)propionic acid) as reference. 1D NOE enhancement experiments were performed in 90% H_2O with a 1:1 jump and return pulse sequence[51] for solvent suppression and a sweep width of 10 000 Hz. In the 2D experiments the H_2O resonance was suppressed by CW irradiation for 1.5 s, and the sweep width was 5000 Hz. The program Felix (Biosym Technologies, San Diego, CA) running on a Silicon Graphics Iris Crimson Elan workstation was used to process the NMR data. The DQF-COSY spectra[52] contained 256 and 2048 complex points in the t_1 and t_2 dimensions, respectively. Initial processing included apodization in both dimensions with a sine squared function shifted by 45° and zero filling to 512 points in the t_1 dimension. The P. COSY (E-COSY type) spectra[25] contained 512 and 2048 complex points and were acquired with a mixing pulse of 35°. NOESY spectra were obtained at mixing times (τ_{mix}) of 100 and 300 ms. A composite 180° pulse (90_x, 180_y, 90_x) in the middle of the mixing period improved solvent suppression, and 5 ms homospoil pulses were used at the beginning of τ_{mix} and after the composite 180° pulse.[53] The NOESY spectra consisted of 512 and 2048 complex points in the t_1 and t_2 dimensions, respectively; the spectra were apodized with a 3 Hz exponential in t_1 and a 90° shifted sine bell in t_2, t_1 was zero-filled to 1024 points.

Analysis of NMR Data. Resonance assignments of Zn(II)·BLM A_2, Zn(II)·BLM A_5, and the octanucleotide $d(CGCTAGCG)_2$ were derived from assessment of the DQF-COSY and NOESY ^1H NMR experiments. With the exception of minor variations in chemical shifts due to temperature and solvent composition, resonance assignments for Zn(II)·BLM A_2[18] and $d(CGCTAGCG)_2$[54] were in agreement with those previously reported. Chemical shifts for Zn(II)·BLM A_5 were similar to those for Zn(II)·BLM A_2, with the exception of the C-terminal substituent. In the BLM−DNA complexes, intermolecular and intramolecular NOESY cross peak volumes were converted to interproton distances using the two spin approximation ($r_{ij} = r_{ref}(R_{ref}/R_{ij})^{1/6}$). The cytidine H5-H6 distance of 2.45 Å was used for calibration (r_{ref}).[55] Intramolecular BLM−BLM and DNA−DNA distances were obtained from the 100 ms mixing time NOESY spectra and were classified semiquantitatively into three categories: strong (1.80−2.5 Å), medium (between 2.51 and 3.7 Å), or weak (3.71−5.0 Å). The intermolecular BLM−DNA distances were acquired from both NOESY spectra (300 ms and 100 ms) and were given a wider range (between 2.0 and 4.70) due to the uncertainty in the derived distances. For methyl and methylene protons, another 1 Å was added to the upper bound of the restraints to compensate for center averaging. From the E.COSY type spectrum, J coupling constants for the H1′−H2′ and H1′−H2″ of the deoxyribose sugars were measured. Qualitative estimation of the pseudorotation angle ranges for the deoxyribose sugars of the octanucleotide were obtained from the DQF-COSY spectra.

DNA Restraints. In addition to the experimentally derived distance and dihedral restraints obtained from the NMR data, four other types of restraints were used in calculating the structures presented in this study. To preserve the right-handed character of the DNA duplex during the molecular dynamics calculations, the α, β, γ, ϵ, and ζ backbone torsion angles were restrained to a range covering both right-handed A and B-DNA.[56] To avoid collapse of the major groove during the high temperature dynamics phase of the simulation, C1′ atoms on opposite sides of the major groove were restrained to be greater than 16.0 Å apart during the calculation.[57] Base pairs were kept Watson−Crick hydrogen bonded by using distance restraints between the bases.[56b] Each base pair was also constrained to be coplanar by applying dihedral angle restraints. In all, for modeling the Zn(II)·BLM A_5−$d(CGCTAGCG)_2$ complex, 8 intermolecular BLM−DNA NOE restraints, 18 nonvicinal BLM - BLM NOE restraints, 210 DNA−DNA NOE restraints, 34 DNA−DNA distance restraints, 159 DNA−DNA dihedral angle restraints, 19 BLM chiral restraints, and a cytidine$_7$ H4′−metal ion restraint (between 2 and 6 Å) were used. Listings of restraints are available as supplementary material (Tables 2, 3, and 5).

Molecular Modeling. Modeling of the interaction of Zn(II)·BLM with the octanucleotide $d(CGCTAGCG)_2$ was performed using the Insight II/Discover program and the Biosym CVFF force field. Heme parameters provided with Insight II were used to model BLM−metal ion interaction. The five BLM ligands identified previously were arranged around the metal in a square pyramidal arrangement, with the Man carbamoyl as the axial ligand. The octamer $d(CGCTAGCG)_2$ was constructed in a standard B-form using Insight II. To provide a starting structure of the BLM−DNA complex, the BLM was docked

(49) Nightingale, K. P.; Fox, K. R. *Nucleic Acids Res.* **1993**, *21*, 2549.
(50) Wilson, W. D.; Tanious, F. A.; Barton, H. J.; Strekowski, L.; Boykin, D. W. *J. Am. Chem. Soc.* **1989**, *111*, 5008.
(51) Plateau, P.; Guéron, M. *J. Am. Chem. Soc.* **1982**, *104*, 7310.
(52) Piantini, U.; Sorensen, O. W.; Ernst, R. R. *J. Am. Chem. Soc.* **1982**, *104*, 6800.
(53) Blake, P. R.; Park, J. B.; Bryant, F. O.; Aono, S.; Magnuson, J. K.; Eccleston, E.; Howard, J. B.; Summers, M. F.; Adams, M. W. W. *Biochemistry* **1991**, *30*, 10885.
(54) Pieters, J. M. L.; de Vroom, E.; van der Marel, G. A.; van Boom, J. H.; Altona, C. *Eur. J. Biochem.* **1989**, *184*, 415.
(55) Baleja, J. D.; Moult, J.; Sykes, B. D. *J. Magn. Reson.* **1990**, *87*, 375.
(56) (a) Gronenborn, A. M.; Clore, G. M. *Biochemistry* **1989**, *28*, 5978. (b) Baleja, J. D.; Pon, R. T.; Sykes, B. D. *Biochemistry* **1990**, *29*, 4828.
(57) Huang, P.; Eisenberg, M. *Biochemistry* **1992**, *31*, 6518.

into the minor groove of the B-form octamer using the simulated annealing protocol[58] that included the BLM−DNA and BLM - BLM distance restraints. The B-form octamer was restrained during the annealing using a template force constant of 10000 kcal/Å. The resulting structure was utilized as a starting point for the restrained molecular dynamics calculations.

The protocol of restrained dynamics was similar to the one employed by Mujeeb et al.[59] and more recently by Schweitzer and co-workers.[23] The starting BLM−DNA structure was first energy minimized with 100 steps of steepest descents, followed by 500 cycles of conjugate gradient minimization with k_{NOE} at 0.5 kcal·mol^{-1}·Å^{-2} and k_{CDIH} (dihedral restraint constant) at 5.0 kcal·mol^{-1}·rad^{-2}. The system was then slowly heated to 1000 K. During this high temperature phase of the simulation, k_{CDIH} was constant at 50.0 kcal·mol^{-1}·rad^{-2}, k_{NOE} was slowly increased from 0.5 to 25 kcal·mol^{-1}·Å^{-2}, and the relative weights of all force field energy terms were reduced to 25%. The system was then gradually cooled to 300 K, and the weights of the force field energy terms were restored to full scale. For the annealing, the dynamics integration time step was 1 fs, the cutoff distance for nonbonded interactions was set at 10 Å with a switching distance of 2 Å, and a distance dependent dielectric of $\epsilon = r_{ij}$ was used. Ten final structures, all of which satisfied the distance restraints to within 0.3 Å, were energy minimized using 30 000 cycles of conjugate gradient minimization to a final root mean square derivative of <0.001 kcal·mol^{-1}·Å^{-2}. The effect of solvent was approximated by a distance dependent dielectric of $\epsilon = 4r_{ij}$ and by reducing the net charge on the phosphate group to −0.32e.[60] A formal charge of 2+ was assigned to the metal ion of BLM and primary amines were protonated.

Acknowledgment. This study was supported by Research Grant CA53913 from the National Cancer Institute.

Supporting Information Available: Tables of coupling constants, torsion angles, hydrogen bond distance constraints, atomic RMS differences between structures obtained by molecular dynamics calculations on Zn(II)·BLM A_5−d(CGCTAGCG)$_2$, and intermolecular drug-DNA NOE contacts for Zn(II)·BLM A_5−d(CGCTAGCG)$_2$ and spectra of free octanucleotide and d(CGCTAGCG)$_2$ plus Zn(II)·BLM A_5, DQF-COSY ^{1}H NMR spectrum of Zn(II)·BLM A_5−d(CGCTAGCG)$_2$, overlay of calculated structures of Zn(II)·BLM A_5−d(CGCTAGCG)$_2$, plot of global helical roll angle as a function of base step for the free octanucleotide versus Zn(II)·BLM A_5 bound octanucleotide, and plot of global helical twist angle as a function of base step for the free octanucleotide versus Zn(II)·BLM A_5 bound octanucleotide (11 pages). This material is contained in many libraries on microfiche, immediately follows this article in the microfilm version of the journal, can be ordered from the ACS, and can be downloaded from the Internet; see any current masthead page for ordering information and Internet access instructions.

JA950820P

(58) Nilges, M.; Clore, G. M.; Gronenborn, A. M. *FEBS Lett.* **1988**, *229*, 317.

(59) Mujeeb, A.; Kerwin, S. M.; Kenyon, G. L.; James, T. L. *Biochemistry* **1993**, *32*, 13419.

(60) Tidor, B.; Irikura, K. K.; Brooks, B. R.; Karplus, M. *J. Biomol. Struct. Dyn.* **1983**, *1*, 231.